Future prospects for biomolecular trapping with nanostructured metals

Reuven Gordon*

Department of Electrical and Computer Engineering, University of Victoria, Victoria, BC, V8P3W6

E-mail: rgordon@uvic.ca

Abstract

Optical trapping with nanostructured metals has allowed for label-free tether-free analysis of single proteins (and other biomolecules) and their interactions with fast detector limited time resolution and duration extending to hours. This perspective will provide a brief historical introduction, discuss recent advances to augment the technique with other approaches, and discuss potential for improved performance and widescale adoption in a range of applications from biologics and drug discovery to fundamental biophysical studies.

Introduction

Label-free single-molecule sensing is a primary emerging area of biotechnology. The aim is to understand how proteins function, rapidly find biologics of interest, accelerate the discovery of drugs and detect with extreme sensitivity. While there has been great impact from single molecule techniques using labels and/or tethers,[1] label-free means that we try not to alter the characteristics of the biomolecules under observation, nor do we rely on time-consuming

and costly labels. Label-free also means we are measuring a direct signal molecule rather than the indirect signal from the labels, and we can observe for a long time as well as at fast time scales (even shorter than nanoseconds) since we are not limited by the timescales associated with the label. Single-molecule means we can observe dynamics in real-time, we can work with unprocessed "dirty" solutions and we can observe heterogeneity in behavior. Single molecule also means that we can observe dynamics at equilibrium, such as on-off binding.

There have already been successes in commercializing single molecule approaches, such as nanopores to sequence DNA.[2] Recently, there have been approaches to use a nanopore electro-osmotic trap (NEOtrap) to size proteins[3] based on changes in ionic current flowing through the pore. Proteins can also be sized by light interference scattering (iScat),[4,5] as well as their dynamics monitored.[6] These pioneering approaches lead the way to a suite of future single molecule tools that provide richer information than existing approaches and can be applied to many existing applications as well as new ones.[7]

Optical tweezers use light to hold onto nanoscale objects.[8] To trap nanoparticles with conventional optical tweezers requires watts of laser power focussed down to the diffraction limited length-scale of around a micron, which can be damaging, but also provides a fairly large trap that can contain many nanoscale objects at once – therefore it does not really allow for isolation of biomolecules. Nanostructured metals (commonly called plasmonics or nanoplasmonics) allow for confining the beam to sizes below the diffraction limit, comparable to single proteins. This offers the potential for trapping and observing single proteins, or other biomolecules and their interactions, in solution.

This perspective piece will discuss the use of nanostructured metals, particularly apertures in metal films, for label-free and tether-free single molecule studies. The ability to hold onto single molecules without tethers and to measure their properties without labels is what makes this approach particularly attractive. Recent demonstrations have shown the utility of this approach to monitor proteins and their interactions, and lead the way to promis-

ing applications, ranging from drug discovery to antibody screening. Internationally, there are about 20 research groups that are working on aperture-based trapping,[9–25] and only a handful of these have trapped single proteins. Even so, there are many recent and detailed works that review plasmonic trapping, some of which already include a detailed discussion of aperture-based trapping and of biological applications.[26–34] In the past few years, however, there have been several breakthrough applications in applying shaped apertures in metal films to the analysis of single proteins and their interactions, and an improvement in the understanding of this system. Therefore, here I will focus on aperture-based techniques for single biomolecule analysis as a potentially disruptive technology of the future.

Nanostructured Metals for Trapping

The pioneering work on trapping nanoparticles with focused laser beams recognized that several watts of focused laser power are required to hold onto particles substantially less than 100 nm in size.[8] This led to theoretical predictions in 1997 that suggested a sharp metal tips could increase the local field intensity by 3000 times, resulting in predicted trapping of 10 nm dielectric spheres with only 6.5 mW of total incident power.[35] Showing particular foresight, that work focused on non-resonant excitation (i.e., away from plasmonic resonances) to avoid damage. Even so, the local heating was predicted to increase the temperature by 6.5 K at the surface of the metal. Fortunately, the sharp metal tip benefits from the thermal conductivity of the gold, 500 times greater than that of the surrounding water, to remove heat, whereas it is known that isolated metal nanostructures at the plasmonic resonance create substantial local heating.[36] Figure 1 shows the calculated local field intensity at a metal tip, and the corresponding temperature increase.

Apertures in metal films for trapping nanoparticles were investigated theoretically in 1999,[37] and later demonstrated on colloid-lithography fabricated structures.[9] In 2009, it was recognized that this trapping was more efficient due to self-induced back-action, where the

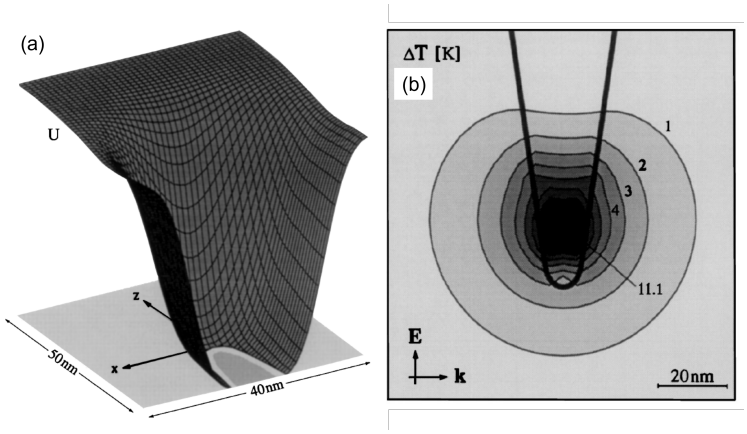

Figure 1: (a) Optical potential of a 10 nm diameter particle of permittivity 2.5 near a sharp metal tip in water. The potential minimum is approximately 25 times the thermal energy for intensity of 1 W/μm^2. (b) Corresponding temperature increase for 65 mW/μm^2 incident intensity. Adapted from Ref.[35] 1997 ©APS.

particle significantly alters the electromagnetic field distribution and makes the trapping more efficient.[11] This allowed for trapping of 100 nm particles with less than 1 mW of power.[11] An important feature of this technique is that the trapping was easily monitored by measuring jumps in the transmission of the laser through the aperture – thus providing a simple label-free way of detecting the trapping events not found in previous works. The surrounding metal film also assisted in removing heat – some have calculated that this gives four orders of magnitude less heating than corresponding isolated metal nanostructures with comparable local field enhancement.[38]

Going beyond simple circular apertures, shaped apertures were used to localize the field further and thereby achieve trapping of 12 nm silica spheres[10] and single proteins,[39] while still benefiting from simple detection by monitoring jumps in transmission. In those works double nanoholes (DNHs), combining two single nanoholes, were used. (It should be noted that earlier works using nanoantennas reported trapping of 10 nm gold particles, but not for dielectric particles[40]).

Similarly, shaped apertures have been used to trap quantum dots[13] and use them as single photon emitters,[41] as well as to re-position fluorescent beads[42] by forming the aperture at the end of a tapered fiber. Various shapes have been explored, like rectangles,[43]

bowties,[13,16,17,22,42] Fano resonant asymmetric apertures[25] and coaxial apertures.[24,44,45] Even algorithm designed apertures have been realized for improved trapping using the double-nanohole as a starting point.[20] Common to all these structures is that the aperture shape should contain a narrow gap or sharp features which localizes the field further for trapping, which was not afforded by the circular shape of earlier works. Figure 2 shows a composite of various apertures that have been investigated.

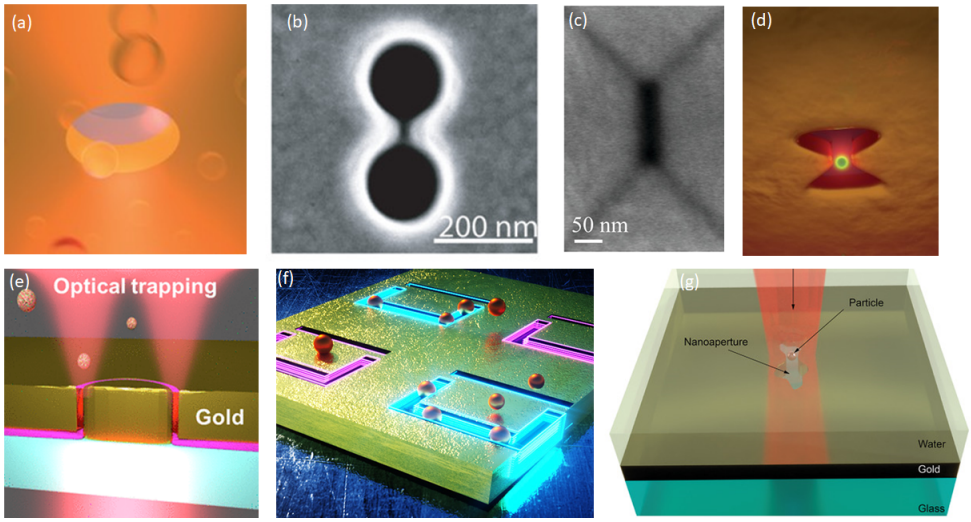

Figure 2: Various apertures for label-free trapping. (a) Circular (reprinted as co-author[11]). (b) Double Nanohole (Reprinted (adapted) with permission from.[10] Copyright 2011 American Chemical Society). (c) Rectangular (Reprinted (adapted) with permission from.[43] Copyright 2011 American Chemical Society). (d) Bowtie . (e) Coaxial (Reprinted (adapted) with permission from.[24] Copyright 2018 American Chemical Society). (f) Composite (Fano) (Reprinted with permission of author[25]). (g) Algorithm designed.

The double-nanohole structure can be fabricated by inexpensive colloidal methods[46] and identified and oriented without the need for electron microscopy or ion beam milling.[47] This makes the approach accessible to anyone that has a common laser tweezer setup and the facilities to evaporate thin metal films. Therefore, aperture-based optical tweezers for single protein analysis have become a tool broadly accessible to researchers without any specialized facilities or advanced nanofabrication.

Physical Considerations

Even without labels or tethers, analysis of single biomolecules and their interactions involves perturbing them away from their native environment. For nanopore technologies, the largest perturbation involves working at salt concentrations that are an order of magnitude higher than physiological conditions.[48] Nanostructured metals for optical tweezers have an operating environment with a strong local field, local field gradient, surfaces and local heating. We consider the operating environment in the context of analysis of biomolecules with optical tweezers.

Proteins

Since this work is mainly considered with proteins, it is useful to briefly review some of their physical properties that are relevant for trapping in a solution. There are different types of proteins: membrane, disordered, globular, and fibrous proteins. These exist in membranes, as part of ordered fibers and in free-solution. The median length of human proteins is 375 amino acids,[49] or approximately 50 kDa. The approximate diameter of this median length protein is 5 nm diameter. There are of the order of 100,000 different proteins in the body, and they can exist in close proximity. For example, the density of albumin in the blood is typically around 4 g/dL, which means that the average separation between two of these is only around 100 nm.

Typical salt concentrations in the body are around 150 mM,[3] and the composition in cells is different. Physiological pH is around 7.4. The refractive index of proteins has been suggested to be around 1.45,[50] but it is known to be dependent size, shape, environment.[51] When dealing with optical tweezers, it is important to account for thermophoretic effects – proteins can either be attracted to heat or cold and this depends on temperature and salt concentration.[52] At physiological conditions, proteins are typically thermophobic, but they can be thermophilic at lower temperatures.[53] Proteins can be denatured by changes in pH,

heating and interactions with chemicals like urea and ethanol.[54] They can also be denatured by the addition of surfactants.[55] Therefore, an ideal trapping environment will be as close to physiological conditions as possible and could be aided by thermophoresis.

Interaction with the Electric Field

The potential energy associated with trapping a nanoparticle in the dipole limit is given by:

$$U = -\frac{1}{2}\vec{p}\cdot\vec{E} \tag{1}$$

where $\vec{p}$ is the dipole moment and $\vec{E}$ is the electric field. Interestingly, the dipole itself becomes polarized and so its energy increases; however, the total energy decreases by an equal amount to give a a potential minimum at the highest field intensity location.[56] The optical potential should be greater than the thermal energy, k_BT (where k_B is Boltzmann's constant and T is temperature in Kelvin), to stably trap the particle.[8]

The polarizability of a prolate spheroid (an approximate shape for a globular protein) is:

$$\alpha = \frac{V\epsilon_0\left(\epsilon_d - \epsilon_b\right)}{A\left(\epsilon_d - \epsilon_b\right) + \epsilon_b} \tag{2}$$

where V is the volume of the particle and ϵ_0 is the free-space permittivity and A is a geometric factor:

$$A = \left(\xi^2 - 1\right)\left(\frac{\xi}{2}\ln\left[\frac{\xi+1}{\xi-1}\right] - 1\right) \tag{3}$$

where $\xi = a/\sqrt{a^2 - b^2}$ and a and b are the long and short axes, with $A = 1/3$ for a sphere. Since $\vec{p} = \alpha\vec{E}$ using these values, we find that 10^{14} W/m^2 is the beam intensity required to trap a 5 nm diameter sphere with $\epsilon_d = 2.25$ and the surrounding water relative permittivity $\epsilon_b = 1.77$. This is equivalent to a 100 W laser beam focused down to a micrometer squared. For a metal nanostructure, the equivalent power would be 10 mW beam focussed down to 100 nm^2.

Back-Action

The protein or nanoparticle can influence the field, and thereby change the overall potential through Eq. 1. A strongly resonant system, like a photonic crystal, allows for shifting the resonance frequency and changing the energy stored with the introduction of a particle.[57] Photonic crystals have been used for trapping fairly large labelled single proteins (monitored by fluorescence).[58] Around 10 mW of power was coupled into the cavity (although with a quality factor of several thousand, the intensity is expected to be 3-4 orders of magnitude larger inside the cavity, which is similar to the analysis above for powers required to trap). In photonic crystals, the particle can be treated as a dipole still, not significantly changing the field profile and therefore not requiring Maxwell stress tensor analysis.[57] By contrast, in apertures in metal films the force calculated with Maxwell stress tensor analysis was significantly larger,[11] showing clearly the impact of the particle on the trapping potential (i.e., back-action) not considered in other works.[9,37]

The particle itself may also play a negative role in reducing the trapping potential by shifting the plasmonic resonance away from the trapping laser wavelength.[59] As a result, negative steps in the optical transmission through the aperture can be observed.

Elongation, Orientation and Size-Effects

Using the same approach as above with Eq 2, we can estimate how much the potential energy changes in deforming the particle. This is important because the optical tweezer will act to elongate or stretch the protein through the process of electrostiction, and this may be considered an unwanted perturbation from the protein's natural state. To understand the magnitude of this deformation, a 10% increase in the length of the particle along one axis from a sphere to a spheroid (without changing the refractive index or the volume, to first order) gives a potential energy change is 1%. Therefore, the electrostriction force may be considerably smaller than k_BT, the thermal energy, while still having stable trapping. The elastic response will act against electrostriction to minimize deformation. In the case where

the particle gives a negative step in the aperture transmission, this will act to reduce the field intensity and minimize electrostriction effects, even though stable trapping can still be achieved.[59]

In the first trapping studies of bovine serum albumin (BSA) trapping in a DNH,[39] BSA showed elongation with an increase in optical transmission through the aperture (transitioning from the N-form to the F-form). The protein did transition back to the F-form, which suggests that the potential energy to elongate the protein was comparable to energy that kept it in the N-form. (The elongation was confirmed by forcing the BSA into the F-form with decreased pH).

Similarly, studies on trapping of 20 base DNA hairpins in DNHs showed unzipping (elongation) of the DNA hairpin after trapping,[60] which was irreversible. Forces of this unzipping process are of the order of 10 pN and over this lengthscale, it is estimated to be slightly larger than the thermal energy. Doubling the length of the DNA, while halving its cross-section approximately doubles the polarizability – so the transmission through the DNH doubled with this elongation (according to Eq. 1 this doubling is expected). There is also an entropic penalty associated with zipping, and so this process is somewhat more complicated.

The polarizability along the long axis is the highest and so there is torque orienting the particle along this axis; however, in some cases steric hindrance will favor a different orientation. For example, it was calculated that close to a sharp tip the particle will orient along its short axis because then it can have the greatest overlap with the high intensity region of the electromagnetic field.[35]

For plasmonic trapping, the centre of a bigger particle is not as close to the highest intensity at the surface, and so there signal is reduced (as compared to the scaling expected for free-space scattering) and the bigger particle experiences a reduced trapping potential.[61] Here it is suggested that this leads large particles, like 20 nm polystyrene spheres, to have a similar change in transmission to smaller particles, like single proteins.[10,39] Therefore, it is suggested that measuring particle size from step heights may only be suitable for smaller

particles.

Thermal Effects

Thermal effects play a role in trapping biomolecules with nanostructured metals because they can adversely affect the biomolecule and influence the trapping efficiency. Simulations of heating in DNH apertures and tracking of particle motion estimated around 1K increase per mW/μm^2 of incident intensity.[19] Analysis of DNH apertures with fluorescence showed a larger 2 mW/μm^2 produced 10 K increase in temperature;[15] however, this heating was also shown to be strongly dependent on substrate thermal conductivity, adhesion layer absorption and illumination direction (from the adhesion layer side or not).[62] For example, four times lower heating was observed by illuminating from the opposite side of the adhesion layer, which is consistent with other works.[16] By using sapphire as the substrate, 17 times lower heating was observed.[62] This heating has been modelled extensively and is well-understood.[63] As a complementary approach, analysis of temperature increases in bowtie apertures showed 3.6 K increase in temperature for 7.5 mW of 1064 nm laser illumination, measured using changes in ionic current through a co-located nanopore.[16] Simulations predicted a value of 3.1 K. Therefore, the literature is largely consistent on the level of heating. It should be noted that monitoring proteins at physiological temperatures (e.g., 310 K for humans) would require substantially larger heating than observed from the laser alone, and so this would require introducing plasmonic heating or a thermally controlled trapping platform.

While stronger heating has been used to induce flows and assist transport with metal particle and aperture array based systems,[23,64,65] the level of heating is not enough with a single aperture to produce any significant flows; about 10 nm/s is predicted for intense 10mW/μm^2 excitation.[19]

In addition to the absolute temperature, the heating occurs in a localized region which leads to large thermal gradients and thermophoresis.[18] While it is possible to change the thermophoretic properties by suitable choice of surfactant,[18] this can lead to denaturing of

proteins. Even so, thermal gradients can assist trapping since the Soret coefficient for many proteins is typically negative for lower temperatures, but positive (repelling) for physiological temperatures. This means that one may have to trap at a lower temperature, then increase temperature. Alternatively, nanopore approaches can be used to flow the protein to the trapping region.[12,17]

Surface Interactions and Diffusion

In aqueous solution, the nanoparticles and the surfaces typically have negative charge, and so the nanoparticles are repelled from the surface. By changing the geometry, this charge can be used to trap particles away from a surface in a controllable way without light.[66] This also serves to minimize surface fouling. At the same time, this acts against the optical trapping potential, and makes the time-to-trap longer.[67] A simple estimation of the time-to-trap would suggest that without surface repulsion the time-to-trap would be of the order of milliseconds at typical concentrations used, yet the actual time observed in experiments is of the order of minutes. To further support this hypothesis, trapping of inorganic particles in hexane, which does not have this surface repulsion, was observed to be in the expected millisecond range.[68,69]

While surface repulsion can be annoying by creating a delay in trapping, it also prevents interactions with the surface (including corrections to drag that were originally thought to be important[70]). The combination of the optical potential and the electrostatic potential creates a stable minimum away from the surface and so trapping occurs essentially in free solution. Detailed analysis of the dynamics including these surface charges is an area for further investigation.[71]

Single Proteins?

The uniformity of step height in trapping is an indication that only a single protein was trapped.[39] In the early protein trapping work, BSA underwent a conformation change, so it

was important to rule out that the double-step observed was not coming from trapping of two proteins, which was done by forcing the BSA into a different conformation where only a single step was observed. Such changes in state of a protein in a trap have been observed by others.[72]

When multiple nanoparticles are trapped in an aperture-based trap, a double-step is observed.[43] We showed that this double-step (double trapping) occurs very infrequently for proteins.[73] We believe this is because proteins carry a slight charge and repel each other in solution; therefore, it is unlikely to have two in the same trap unless they have some attractive interaction. Furthermore, we can size the proteins accurately based on their trapping signal, and so we know even the precise size of the protein trapped,[74] let alone that it is a single entity.

Works combining aperture trapping with nanopores have a complementary ionic current signal, which only goes further to verify that this is"nano-optical trapping of single proteins" .[17,75]

Applications to Studying Proteins and other Biomolecules

Aperture optical tweezers can used to observe single proteins, other biomolecules and their interactions in a label-free, tether-free way.[30] Among the studies so far are:

- specific binding of antibodies to antigen (protein) targets[12,76]
- quantifying low-affinity interactions with small molecules[77] and biologics[75]
- measuring protein-protein interactions (e.g., the mass change with tryptic cleaving of serpines[74])
- measuring high-affinity binding interactions to small molecules[78]
- sizing proteins[74]

- measuring the low-frequency normal modes of proteins,[79] DNA[80] and even entire virus particles[81]
- measuring protein-DNA interactions (e.g., comparison between wild-type and mutant p53 binding to DNA[60]
- measuring concentrations of various proteins in unprocessed (dirty) samples[73]

In addition, the nanoapertures also enhance the Raman signal from the particle in the aperture and so this can be used in identification.[21,82] It is possible that this could lead to direct reading of DNA bases with apertures using their natural Raman scattering response,[83] where the aperture slows down the translocation speed to improve performance. Metal nanoparticle based antennas have significant heating since they are thermally isolated, so this tends to negate the optical tweezer's effect to slow down translocation,[84] as compared with aperture-based tweezers where a clear slowing down was observed.[14,17]

Comparing and Combining with Other Approaches

Sensitivity in Sizing

Figure 3 shows the measured protein size published for iScat,[5] NEOtrap[3] and the DNH optical trap.[74] The signal measured is different in each case. With iScat, it is the related to the scattering, so the polarizability of the protein. For NEOtrap, it is the change in ionic current using a protein trapped in a nanopore. For the DNH, it is the fluctuations in signal that come from the motion of the protein in the trap. This fluctuation actually gives two independent measures of the protein size – from the amplitude and the time-scale of the fluctuation. As described previously, the amplitude scales linearly with particle size and the time constant of the autocorrelation scales with a -2/3 power.[74]

All three approaches show good linearity, however, it appears that so far iScat and NEOtrap have been applied mainly to proteins larger than 50 kDa, whereas the DNH has

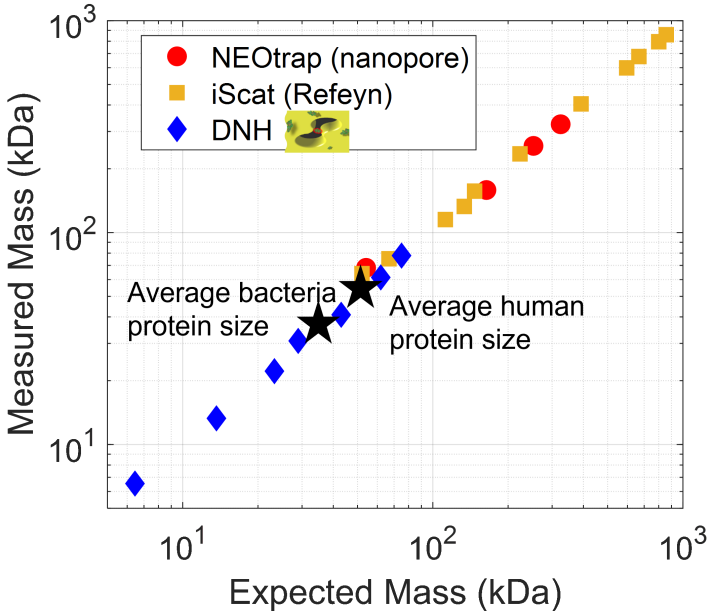

Figure 3: Various proteins measured by 3 different techniques. NEOtrap uses a nanopore obstruction and monitors ionic current.[3] iScat (being commercialized by Refeyn) uses interference scattering.[5] The DNH uses thermal motion of a trapped particle.[74] The NEOtrap and iScat have been demonstrated down to the average human protein size, whereas the DNH extends down to below 10 kDa.

probed down to 6.5 kDa. This is an important distinction considering that the median human protein size is close to 50 kDa,[49] and the median bacteria protein size is 70% of this value. Clearly to probe the smallest proteins, it is desirable to have a limit of detection below 10 kDa. Obviously there are many other dimensions in which to compare these different approaches, considering how they monitor complexes, conformations, dynamics, types of proteins, speed of analysis, ease of use etc. These approaches are all in the early stages and each show promise as complementary ways in the increasingly important area of single molecule analysis. For example, it is possible that sensitivity of optical approaches (including iScat) will improve substantially with the introduction of quantum-based detection.[85]

Aperture Tweezers and Nanopores

Two groups have combined aperture tweezers with nanopores to obtain complementary ionic current and optical signals.[12,14,16,17,75] Figure 4 shows a comparison between ionic current,

ionic translocation time, optical trapping time and optical step height used to distinguish between an antigen and an antibody. It was found that the optical step change "provided the clearest separation between antigen and antibody" and so that was used in the subsequent analysis.[12] It should be noted that other optical signals, such as the autocorrelation response or the noise amplitude, were filtered out in that work, and could provide further analytic capability in the future.

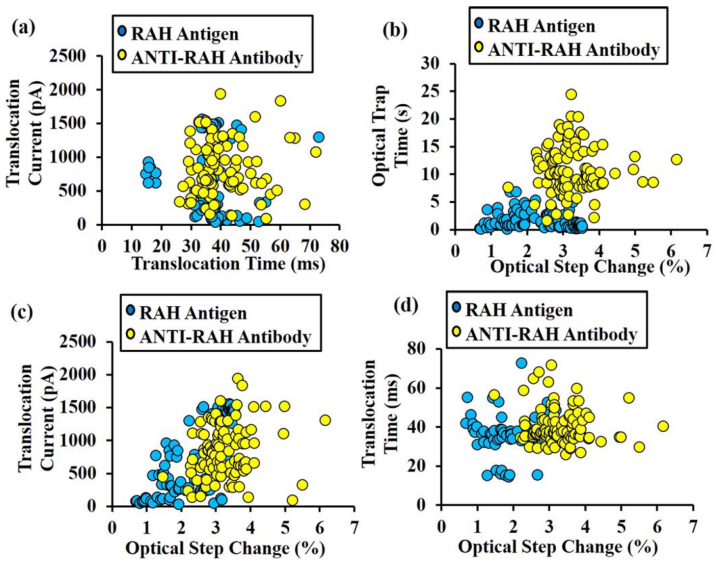

Figure 4: Comparison of detection events of RAH antigen (300 nM) and its antibody (300 nM) using (a) nanopore translocation current and time, (b) double-nanohole optical step height and optically-detected trap time, (c) combined nanopore current and optical step height, and (d) combined nanopore translocation time and optical step height change. From this analysis, it was determined that the optical step height change gave the clearest distinction between RAH and anti-RAH.[12] Reproduced with permission ©IOP 2019.

An important feature of the nanopore work is that it solves the surface repulsion problem of the aperture-based technique by flowing the proteins into the aperture.[17] This is a valuable advance; however, it introduces instrument complexity and depending upon the application it may be better to simply use the nanoapertures.[72] To avoid working at high salt concentrations or using electrokinetic flow, it is possible to use pressure driven flow.[86]

Outlook

The present pandemic, as well as Zika and Ebola outbreaks, have created important application areas for rapid and portable nanopore based DNA sequencers,[87] as compared to dominant fluorescence-based techniques.[88,89] The value of this technology is apparent: after initial public offering in September 2021, Oxford Nanopore now has a market capitalization of 4.33B pounds. There is a growing concensus that techniques that allow for the analysis of single proteins will be similarly valuable in the near future.[7,90] Ideally, these techniques should be label-free and tether-free to avoid disruption of the protein. They should also operate in as close to physiological conditions as possible, to observe the protein's natural behavior and interactions in real time. With this capability, it is possible to watch proteins at work with minimal solution purification or preparation (i.e., one may start with unprocessed "dirty" solutions). This has many applications in discovering small molecule drugs and biologics, ultrasensitive detection, as well as understanding the basic nature of proteins and their interactions.

Accessibility and scalability of aperture-based tweezers is likely to be a key part of future developments. Scalability may come from integrating the aperture based tweezers on the ends of multiple fibers.[42,91,92] In this way, it may be possible to address multiple well-plates in a way similar to bio-layer interferometry, which has become a popular high-throughput technique.[93] Unlike bio-layer interferometry, the aperture optical tweezer does not require surface tethers/binding, and it operates at the single molecule level. Fabrication complexity and cost has also been a challenge for nanotechnologies; however, colloidal based techniques offer a facile way of creating high-quality DNHs for optical tweezing of proteins and other biomolecules.[46,47] Field induced breakdown may allow for co-locating the DNH with a nanopore,[94] which would greatly simplify this dual-method that has already shown remarkable application to immunotherapy targets.[12,75] Therefore, it is my perspective that recent advances have improved the prospects of this technique becoming a widely used technology.

Acknowledgement

Funding provided by Human Frontier Science Program (RGP0027/2020-ITZHAKI) and Natural Sciences and Engineering Research Council (RGPIN-2017-03830). The author thanks Michael Dobinson for providing the TOC figure.

References

(1) Lipman, E. A.; Schuler, B.; Bakajin, O.; Eaton, W. A. Single-molecule measurement of protein folding kinetics. *Science* **2003**, *301*, 1233–1235.

(2) Howorka, S.; Cheley, S.; Bayley, H. Sequence-specific detection of individual DNA strands using engineered nanopores. *Nature Biotechnology* **2001**, *19*, 636.

(3) Schmid, S.; Stömmer, P.; Dietz, H.; Dekker, C. Nanopore electro-osmotic trap for the label-free study of single proteins and their conformations. *Nature Nanotechnology* **2021**,

(4) Piliarik, M.; Sandoghdar, V. Direct optical sensing of single unlabelled proteins and super-resolution imaging of their binding sites. *Nature Communications* **2014**, *5*, 1–8.

(5) Young, G.; Hundt, N.; Cole, D.; Fineberg, A.; Andrecka, J.; Tyler, A.; Olerinyova, A.; Ansari, A.; Marklund, E. G.; Collier, M. P., et al. Quantitative mass imaging of single biological macromolecules. *Science* **2018**, *360*, 423–427.

(6) Ortega Arroyo, J.; Andrecka, J.; Spillane, K.; Billington, N.; Takagi, Y.; Sellers, J.; Kukura, P. Label-free, all-optical detection, imaging, and tracking of a single protein. *Nano Letters* **2014**, *14*, 2065–2070.

(7) Alfaro, J. A. et al. The emerging landscape of single-molecule protein sequencing technologies. *Nature Methods* **2021**, *18*, 604–617.

(8) Ashkin, A.; Dziedzic, J. M.; Bjorkholm, J. E.; Chu, S. Observation of a single-beam gradient force optical trap for dielectric particles. *Optics Letters* **1986**, *11*, 288–290.

(9) Kwak, E.-S.; Onuta, T.-D.; Amarie, D.; Potyrailo, R.; Stein, B.; Jacobson, S. C.; Schaich, W.; Dragnea, B. Optical trapping with integrated near-field apertures. *Journal of Physical Chemistry B* **2004**, *108*, 13607–13612.

(10) Pang, Y.; Gordon, R. Optical trapping of 12 nm dielectric spheres using double-nanoholes in a gold film. *Nano Letters* **2011**, *11*, 3763–3767.

(11) Juan, M. L.; Gordon, R.; Pang, Y.; Eftekhari, F.; Quidant, R. Self-induced back-action optical trapping of dielectric nanoparticles. *Nature Physics* **2009**, *5*, 915–919.

(12) Peri, S. S. S.; Sabnani, M. K.; Raza, M. U.; Ghaffari, S.; Gimlin, S.; Wawro, D. D.; Lee, J. S.; Kim, M. J.; Weidanz, J.; Alexandrakis, G. Detection of specific antibody-ligand interactions with a self-induced back-action actuated nanopore electrophoresis sensor. *Nanotechnology* **2019**, *31*, 085502.

(13) Jensen, R. A.; Huang, I.-C.; Chen, O.; Choy, J. T.; Bischof, T. S.; Lončar, M.; Bawendi, M. G. Optical trapping and two-photon excitation of colloidal quantum dots using bowtie apertures. *ACS Photonics* **2016**, *3*, 423–427.

(14) Raza, M. U.; Peri, S. S. S.; Ma, L.-C.; Iqbal, S. M.; Alexandrakis, G. Self-induced back action actuated nanopore electrophoresis (SANE). *Nanotechnology* **2018**, *29*, 435501.

(15) Jiang, Q.; Rogez, B.; Claude, J.-B.; Baffou, G.; Wenger, J. Temperature measurement in plasmonic nanoapertures used for optical trapping. *ACS Photonics* **2019**, *6*, 1763–1773.

(16) Verschueren, D. V.; Pud, S.; Shi, X.; De Angelis, L.; Kuipers, L.; Dekker, C. Label-free optical detection of DNA translocations through plasmonic nanopores. *ACS Nano* **2018**, *13*, 61–70.

(17) Verschueren, D.; Shi, X.; Dekker, C. Nano-Optical Tweezing of Single Proteins in Plasmonic Nanopores. *Small Methods* **2019**, *3*, 1800465.

(18) Jiang, Q.; Rogez, B.; Claude, J.-B.; Baffou, G.; Wenger, J. Quantifying the role of the surfactant and the thermophoretic force in plasmonic nano-optical trapping. *Nano Letters* **2020**, *20*, 8811–8817.

(19) Xu, Z.; Song, W.; Crozier, K. B. Direct particle tracking observation and Brownian dynamics simulations of a single nanoparticle optically trapped by a plasmonic nanoaperture. *ACS Photonics* **2018**, *5*, 2850–2859.

(20) Li, N.; Cadusch, J.; Liu, A.; Barlow, A. J.; Roberts, A.; Crozier, K. B. Algorithm-Designed Plasmonic Nanotweezers: Quantitative Comparison by Theory, Cathodoluminescence, and Nanoparticle Trapping. *Advanced Optical Materials* **2021**, *9*, 2100758.

(21) Kerman, S.; Chen, C.; Li, Y.; Van Roy, W.; Lagae, L.; Van Dorpe, P. Raman fingerprinting of single dielectric nanoparticles in plasmonic nanopores. *Nanoscale* **2015**, *7*, 18612–18618.

(22) Yoon, S. J.; Song, D. I.; Lee, J.; Kim, M.-K.; Lee, Y.-H.; Kim, C.-K. Hopping of single nanoparticles trapped in a plasmonic double-well potential. *Nanophotonics* **2020**, *9*, 4729–4735.

(23) Kotnala, A.; Kollipara, P. S.; Li, J.; Zheng, Y. Overcoming diffusion-limited trapping in nanoaperture tweezers using opto-thermal-induced flow. *Nano Letters* **2019**, *20*, 768–779.

(24) Yoo, D.; Gurunatha, K. L.; Choi, H.-K.; Mohr, D. A.; Ertsgaard, C. T.; Gordon, R.; Oh, S.-H. Low-power optical trapping of nanoparticles and proteins with resonant coaxial nanoaperture using 10 nm gap. *Nano Letters* **2018**, *18*, 3637–3642.

(25) Kotsifaki, D. G.; Truong, V. G.; Chormaic, S. N. Fano-resonant, asymmetric, metamaterial-assisted tweezers for single nanoparticle trapping. *Nano Letters* **2020**, *20*, 3388–3395.

(26) Kotsifaki, D. G.; Chormaic, S. N. Plasmonic optical tweezers based on nanostructures: fundamentals, advances and prospects. *Nanophotonics* **2019**, *8*, 1227–1245.

(27) Crozier, K. B. Quo vadis, plasmonic optical tweezers? *Light: Science & Applications* **2019**, *8*, 1–6.

(28) Garoli, D.; Yamazaki, H.; Maccaferri, N.; Wanunu, M. Plasmonic nanopores for single-molecule detection and manipulation: toward sequencing applications. *Nano Letters* **2019**, *19*, 7553–7562.

(29) Han, X.; Sun, C. Plasmonic tweezers towards biomolecular and biomedical applications. *Applied Sciences* **2019**, *9*, 3596.

(30) Gordon, R. Biosensing with nanoaperture optical tweezers. *Optics & Laser Technology* **2019**, *109*, 328–335.

(31) Koya, A. N.; Cunha, J.; Guo, T.-L.; Toma, A.; Garoli, D.; Wang, T.; Juodkazis, S.; Cojoc, D.; Proietti Zaccaria, R. Novel plasmonic nanocavities for optical trapping-assisted biosensing applications. *Advanced Optical Materials* **2020**, *8*, 1901481.

(32) Tan, H.; Hu, H.; Huang, L.; Qian, K. Plasmonic tweezers for optical manipulation and biomedical applications. *Analyst* **2020**, *145*, 5699–5712.

(33) Xin, H.; Li, Y.; Liu, Y.-C.; Zhang, Y.; Xiao, Y.-F.; Li, B. Optical forces: from fundamental to biological applications. *Advanced Materials* **2020**, *32*, 2001994.

(34) Zhang, Y.; Min, C.; Dou, X.; Wang, X.; Urbach, H. P.; Somekh, M. G.; Yuan, X. Plasmonic tweezers: for nanoscale optical trapping and beyond. *Light: Science & Applications* **2021**, *10*, 1–41.

(35) Novotny, L.; Bian, R. X.; Xie, X. S. Theory of nanometric optical tweezers. *Physical Review Letters* **1997**, *79*, 645.

(36) Baffou, G.; Quidant, R. Thermo-plasmonics: using metallic nanostructures as nano-sources of heat. *Laser & Photonics Reviews* **2013**, *7*, 171–187.

(37) Okamoto, K.; Kawata, S. Radiation force exerted on subwavelength particles near a nanoaperture. *Physical Review Letters* **1999**, *83*, 4534.

(38) Melentiev, P. N.; Afanasiev, A. E.; Kuzin, A. A.; Baturin, A. S.; Balykin, V. I. Giant optical nonlinearity of a single plasmonic nanostructure. *Optics Express* **2013**, *21*, 13896–13905.

(39) Pang, Y.; Gordon, R. Optical trapping of a single protein. *Nano Letters* **2012**, *12*, 402–406.

(40) Zhang, W.; Huang, L.; Santschi, C.; Martin, O. J. Trapping and sensing 10 nm metal nanoparticles using plasmonic dipole antennas. *Nano Letters* **2010**, *10*, 1006–1011.

(41) Jiang, Q.; Roy, P.; Claude, J.-B.; Wenger, J. Single Photon Source from a Nanoantenna-Trapped Single Quantum Dot. *Nano Letters* **2021**, *21*, 7030–7036.

(42) Berthelot, J.; Aćimović, S. S.; Juan, M. L.; Kreuzer, M. P.; Renger, J.; Quidant, R. Three-dimensional manipulation with scanning near-field optical nanotweezers. *Nature Nanotechnology* **2014**, *9*, 295–299.

(43) Chen, C.; Juan, M. L.; Li, Y.; Maes, G.; Borghs, G.; Van Dorpe, P.; Quidant, R. Enhanced optical trapping and arrangement of nano-objects in a plasmonic nanocavity. *Nano Letters* **2012**, *12*, 125–132.

(44) Saleh, A. A.; Dionne, J. A. Toward efficient optical trapping of sub-10-nm particles with coaxial plasmonic apertures. *Nano Letters* **2012**, *12*, 5581–5586.

(45) Saleh, A. A.; Sheikhoelislami, S.; Gastelum, S.; Dionne, J. A. Grating-flanked plasmonic coaxial apertures for efficient fiber optical tweezers. *Optics Express* **2016**, *24*, 20593–20603.

(46) Ravindranath, A. L.; Shariatdoust, M. S.; Mathew, S.; Gordon, R. Colloidal lithography double-nanohole optical trapping of nanoparticles and proteins. *Optics Express* **2019**, *27*, 16184–16194.

(47) Hajisalem, G.; Babaei, E.; Dobinson, M.; Iwamoto, S.; Sharifi, Z.; Eby, J.; Synakewicz, M.; Itzhaki, L. S.; Gordon, R. Accessible high-performance double nanohole tweezers. *Optics Express* **2022**, *30*, 3760–3769.

(48) Willems, K.; Ruić, D.; Lucas, F. L.; Barman, U.; Verellen, N.; Hofkens, J.; Maglia, G.; Van Dorpe, P. Accurate modeling of a biological nanopore with an extended continuum framework. *Nanoscale* **2020**, *12*, 16775–16795.

(49) Brocchieri, L.; Karlin, S. Protein length in eukaryotic and prokaryotic proteomes. *Nucleic Acids Research* **2005**, *33*, 3390–3400.

(50) Aragon, S. R.; Hahn, D. K. Polarizability and Kerr constant of proteins by boundary element methods. *Colloids and Surfaces B: Biointerfaces* **2007**, *56*, 19–25.

(51) Khago, D.; Bierma, J. C.; Roskamp, K. W.; Kozlyuk, N.; Martin, R. W. Protein refractive index increment is determined by conformation as well as composition. *Journal of Physics: Condensed Matter* **2018**, *30*, 435101.

(52) Iacopini, S.; Piazza, R. Thermophoresis in protein solutions. *EPL (Europhysics Letters)* **2003**, *63*, 247.

(53) Niether, D.; Sarter, M.; Koenig, B. W.; Fitter, J.; Stadler, A. M.; Wiegand, S. Thermophoresis: The case of streptavidin and Biotin. *Polymers* **2020**, *12*, 376.

(54) Brandts, J. F. The thermodynamics of protein denaturation. I. The denaturation of chymotrypsinogen. *Journal of the American Chemical Society* **1964**, *86*, 4291–4301.

(55) Otzen, D. Protein–surfactant interactions: a tale of many states. *Biochimica et Biophysica Acta (BBA)-Proteins and Proteomics* **2011**, *1814*, 562–591.

(56) Jackson, J. D. *Classical Electrodynamics*; John Wiley & Sons, 2007.

(57) Barth, M.; Benson, O. Manipulation of dielectric particles using photonic crystal cavities. *Applied Physics Letters* **2006**, *89*, 253114.

(58) Chen, Y.-F.; Serey, X.; Sarkar, R.; Chen, P.; Erickson, D. Controlled photonic manipulation of proteins and other nanomaterials. *Nano Letters* **2012**, *12*, 1633–1637.

(59) Mestres, P.; Berthelot, J.; Aćimović, S. S.; Quidant, R. Unraveling the optomechanical nature of plasmonic trapping. *Light: Science & Applications* **2016**, *5*, e16092.

(60) Kotnala, A.; Gordon, R. Double nanohole optical tweezers visualize protein p53 suppressing unzipping of single DNA-hairpins. *Biomedical Optics Express* **2014**, *5*, 1886–1894.

(61) Righini, M.; Zelenina, A. S.; Girard, C.; Quidant, R. Parallel and selective trapping in a patterned plasmonic landscape. *Nature Physics* **2007**, *3*, 477–480.

(62) Jiang, Q.; Rogez, B.; Claude, J.-B.; Moreau, A.; Lumeau, J.; Baffou, G.; Wenger, J. Adhesion layer influence on controlling the local temperature in plasmonic gold nanoholes. *Nanoscale* **2020**, *12*, 2524–2531.

(63) Rogez, B.; Marmri, Z.; Thibaudau, F.; Baffou, G. Thermoplasmonics of metal layers and nanoholes. *APL Photonics* **2021**, *6*, 101101.

(64) Ndukaife, J. C.; Kildishev, A. V.; Nnanna, A. G. A.; Shalaev, V. M.; Wereley, S. T.; Boltasseva, A. Long-range and rapid transport of individual nano-objects by a hybrid electrothermoplasmonic nanotweezer. *Nature Nanotechnology* **2016**, *11*, 53.

(65) Hong, C.; Yang, S.; Ndukaife, J. C. Stand-off trapping and manipulation of sub-10 nm objects and biomolecules using opto-thermo-electrohydrodynamic tweezers. *Nature Nanotechnology* **2020**, *15*, 908–913.

(66) Krishnan, M.; Mojarad, N.; Kukura, P.; Sandoghdar, V. Geometry-induced electrostatic trapping of nanometric objects in a fluid. *Nature* **2010**, *467*, 692.

(67) Kotnala, A.; DePaoli, D.; Gordon, R. Sensing nanoparticles using a double nanohole optical trap. *Lab on a Chip* **2013**, *13*, 4142–4146.

(68) Alizadehkhaledi, A.; Frencken, A. L.; Dezfouli, M. K.; Hughes, S.; van Veggel, F. C.; Gordon, R. Cascaded plasmon-enhanced emission from a single upconverting nanocrystal. *ACS Photonics* **2019**, *6*, 1125–1131.

(69) Alizadehkhaledi, A.; Frencken, A. L.; van Veggel, F. C.; Gordon, R. Isolating nanocrystals with an individual erbium emitter: A route to a stable single-photon source at 1550 nm wavelength. *Nano Letters* **2019**, *20*, 1018–1022.

(70) Al Balushi, A. A.; Kotnala, A.; Wheaton, S.; Gelfand, R. M.; Rajashekara, Y.; Gordon, R. Label-free free-solution nanoaperture optical tweezers for single molecule protein studies. *Analyst* **2015**, *140*, 4760–4778.

(71) Xu, H.; Jones, S.; Choi, B.-C.; Gordon, R. Characterization of individual magnetic nanoparticles in solution by double nanohole optical tweezers. *Nano Letters* **2016**, *16*, 2639–2643.

(72) Yang, W.; van Dijk, M.; Primavera, C.; Dekker, C. FIB-milled plasmonic nanoapertures allow for long trapping times of individual proteins. *iScience* **2021**, *24*, 103237.

(73) Hacohen, N.; Ip, C. J.; Gordon, R. Analysis of egg white protein composition with double nanohole optical tweezers. *ACS Omega* **2018**, *3*, 5266–5272.

(74) Wheaton, S.; Gordon, R. Molecular weight characterization of single globular proteins using optical nanotweezers. *Analyst* **2015**, *140*, 4799–4803.

(75) Peri, S. S. S.; Sabnani, M. K.; Raza, M. U.; Urquhart, E. L.; Ghaffari, S.; Lee, J. S.; Kim, M. J.; Weidanz, J.; Alexandrakis, G. Quantification of low affinity binding interactions between natural killer cell inhibitory receptors and targeting ligands with a self-induced back-action actuated nanopore electrophoresis (SANE) sensor. *Nanotechnology* **2020**, *32*, 045501.

(76) Al Balushi, A. A.; Zehtabi-Oskuie, A.; Gordon, R. Observing single protein binding by optical transmission through a double nanohole aperture in a metal film. *Biomedical Optics Express* **2013**, *4*, 1504–1511.

(77) Al Balushi, A. A.; Gordon, R. A label-free untethered approach to single-molecule protein binding kinetics. *Nano Letters* **2014**, *14*, 5787–5791.

(78) Al Balushi, A. A.; Gordon, R. Label-free free-solution single-molecule protein–small molecule interaction observed by double-nanohole plasmonic trapping. *ACS Photonics* **2014**, *1*, 389–393.

(79) Wheaton, S.; Gelfand, R. M.; Gordon, R. Probing the Raman-active acoustic vibrations of nanoparticles with extraordinary spectral resolution. *Nature Photonics* **2015**, *9*, 68–72.

(80) Kotnala, A.; Wheaton, S.; Gordon, R. Playing the notes of DNA with light: extremely high frequency nanomechanical oscillations. *Nanoscale* **2015**, *7*, 2295–2300.

(81) Burkhartsmeyer, J.; Wang, Y.; Wong, K. S.; Gordon, R. Optical trapping, sizing, and probing acoustic modes of a small virus. *Applied Sciences* **2020**, *10*, 394.

(82) Jones, S.; Al Balushi, A. A.; Gordon, R. Raman spectroscopy of single nanoparticles in a double-nanohole optical tweezer system. *Journal of Optics* **2015**, *17*, 102001.

(83) Chen, C.; Li, Y.; Kerman, S.; Neutens, P.; Willems, K.; Cornelissen, S.; Lagae, L.; Stakenborg, T.; Van Dorpe, P. High spatial resolution nanoslit SERS for single-molecule nucleobase sensing. *Nature Communications* **2018**, *9*, 1–9.

(84) Nicoli, F.; Verschueren, D.; Klein, M.; Dekker, C.; Jonsson, M. P. DNA translocations through solid-state plasmonic nanopores. *Nano Letters* **2014**, *14*, 6917–6925.

(85) Casacio, C. A.; Madsen, L. S.; Terrasson, A.; Waleed, M.; Barnscheidt, K.; Hage, B.; Taylor, M. A.; Bowen, W. P. Quantum-enhanced nonlinear microscopy. *Nature* **2021**, *594*, 201–206.

(86) Eftekhari, F.; Escobedo, C.; Ferreira, J.; Duan, X.; Girotto, E. M.; Brolo, A. G.; Gordon, R.; Sinton, D. Nanoholes as nanochannels: flow-through plasmonic sensing. *Analytical Chemistry* **2009**, *81*, 4308–4311.

(87) Jain, M.; Olsen, H. E.; Paten, B.; Akeson, M. The Oxford Nanopore MinION: delivery of nanopore sequencing to the genomics community. *Genome Biology* **2016**, *17*, 1–11.

(88) Bentley, D. R.; Balasubramanian, S.; Swerdlow, H. P.; Smith, G. P.; Milton, J.; Brown, C. G.; Hall, K. P.; Evers, D. J.; Barnes, C. L.; Bignell, H. R., et al. Accurate whole human genome sequencing using reversible terminator chemistry. *Nature* **2008**, *456*, 53–59.

(89) Eid, J.; Fehr, A.; Gray, J.; Luong, K.; Lyle, J.; Otto, G.; Peluso, P.; Rank, D.; Baybayan, P.; Bettman, B., et al. Real-time DNA sequencing from single polymerase molecules. *Science* **2009**, *323*, 133–138.

(90) Mannar, D.; Saville, J. W.; Zhu, X.; Srivastava, S. S.; Berezuk, A. M.; Tuttle, K. S.; Marquez, A. C.; Sekirov, I.; Subramaniam, S. SARS-CoV-2 Omicron variant: Antibody evasion and cryo-EM structure of spike protein–ACE2 complex. *Science* **2022**, eabn7760.

(91) Ehtaiba, J. M.; Gordon, R. Template-stripped nanoaperture tweezer integrated with optical fiber. *Optics Express* **2018**, *26*, 9607–9613.

(92) Ehtaiba, J. M.; Gordon, R. Beaming light through a bow-tie nanoaperture at the tip of a single-mode optical fiber. *Optics Express* **2019**, *27*, 14112–14120.

(93) Shi, R.; Shan, C.; Duan, X.; Chen, Z.; Liu, P.; Song, J.; Song, T.; Bi, X.; Han, C.; Wu, L., et al. A human neutralizing antibody targets the receptor-binding site of SARS-CoV-2. *Nature* **2020**, *584*, 120–124.

(94) Kwok, H.; Briggs, K.; Tabard-Cossa, V. Nanopore fabrication by controlled dielectric breakdown. *PLOS One* **2014**, *9*, e92880.

Graphical TOC Entry

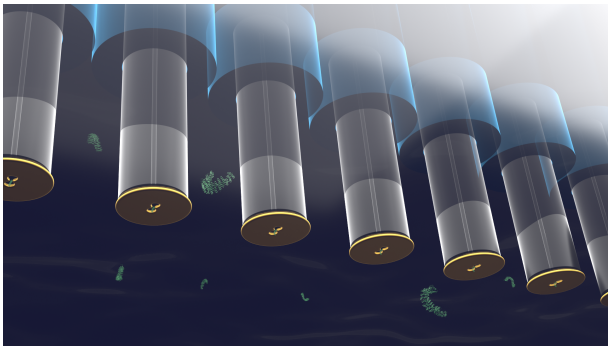

Optical trapping of single proteins in solution using double-nanoholes at ends of optical fibers.